Imaging Acute Cardiac Cell Death: Temporal and Spatial Distribution of ^{99m}Tc-Labeled C2A in the Area at Risk After Myocardial Ischemia and Reperfusion

Xiaoguang Zhu, Zhixin Li, and Ming Zhao

Department of Biophysics, Medical College of Wisconsin, Milwaukee, Wisconsin

The exposure of anionic phospholipids is a near-universal molecular signature for cell death. Based on our prior finding that the ^{99m}Tc-labeled C2A domain of synaptotagmin I accumulates intensely in the area at risk, this study quantitatively characterized the temporal and spatial distribution of the radiotracer in a rat model of myocardial ischemia and reperfusion. **Methods:** Myocardial ischemia and reperfusion were induced by occlusion of the left anterior descending coronary artery in rats. The temporal uptake of the labeled fusion protein of C2A and glutathione-s-transferase (C2A-GST) in the area at risk was investigated by intravenously injecting the radiotracer at 0, 1, 3, 6, and 24 h after reperfusion, and the radioactivity uptake was quantified by γ-counting of infarcted and ischemic noninfarcted cardiac tissues. Alternatively, the radiotracer was injected at 2 h after reperfusion, and the uptake was measured at 1, 3, 6, and 24 h after injection. In vivo planar imaging was performed on a γ-camera using a parallel-hole collimator. The distribution of radioactivity was qualitatively examined by autoradiography. The relationship between the uptake of the radiotracer in the area at risk and the ischemic duration was examined by γ-counting. **Results:** Temporally, the radioactivity uptake in the area at risk maximized when the radiotracer was injected before 3 h after reperfusion. Injections at 6 and 24 h after reperfusion resulted in a 30% and 50% reduction in uptake, respectively. However, when the injection was done early (2 h after reperfusion), the tracer was retained in the area at risk with little washout for at least 24 h. Spatially prominent hot-spot uptake was seen in all cases of planar imaging. In autoradiography, the distribution of radioactivity predominantly coregistered with the infarcted regions. This distribution profile was confirmed by direct γ-counting. In addition, the absolute radiotracer uptake in the infarcted and ischemic noninfarcted tissues, in terms of percentage injected dose per gram, was independent of the ischemic duration. **Conclusion:** ^{99m}Tc-C2A-GST has an uptake profile in the area at risk that is appropriate for imaging cardiac cell death in the acute phase.

Key Words: C2A; synaptotagmin I; apoptosis; necrosis; myocardial infarction

J Nucl Med 2007; 48:1031–1036
DOI: 10.2967/jnumed.106.037754

High levels of cardiac cell death are the primary consequence of severe ischemic injury to the myocardium (*1*) and initiate a vicious cascade that often leads to declined cardiac function and eventual heart failure. In acute myocardial infarction (AMI), the ability to detect the molecular signatures of cell death will facilitate the development of novel imaging tools that offer molecular specificity. Such technologies, in turn, will help us better understand the dynamics of cardiac cell death and validate experimental cardioprotective treatments.

Cardiac cell death induced by ischemia/reperfusion includes both apoptosis and necrosis (*2,3*). Although the former is an energy-dependent intracellular enzymatic process, necrosis is a form of passive cell death recognized by swelling and plasma membrane damage (*3–8*). Although the exact extent to which each form of cell death contributes to AMI remains controversial, the overall irreversible myocardial damage is likely a reflection of all modes of cell death.

A common molecular signature for both apoptosis and necrosis is the exposure of anionic phospholipids, including phosphatidylserine and phosphatidylinositides. Both types of phospholipids are components strictly of the inner leaflet of the plasma membrane. During apoptosis, the compromise of phospholipid asymmetry is accompanied by the exposure on the cell surface of phosphatidylserine, which is recognized by scavenging mechanisms for prompt removal of the dying cell without causing inflammatory responses (*9–11*). In necrotic cells, the passive rupture of the plasma membrane renders intracellular components, including the anionic phospholipids, accessible to the extracellular milieu. Once exposed, the anionic phospholipids provide an abundant molecular marker for the detection of both apoptosis and necrosis.

Received Oct. 31, 2006; revision accepted Mar. 6, 2007.
For correspondence or reprints contact: Ming Zhao, PhD, Department of Biophysics, Medical College of Wisconsin, 8701 Watertown Plank Rd., Milwaukee, WI 53226.
E-mail: mzhao@mcw.edu

Using naturally occurring membrane-binding proteins, molecular probes have been under development for the noninvasive imaging of acute cell death. Among these, annexin V recognizes membrane-bound phosphatidylserine with high affinity and specificity (*12*). Derivatives of annexin V have been demonstrated in the detection of apoptosis in a wide range of model systems (*13–20*). Another protein, the C2A domain of synaptotagmin I, also binds phospholipid membranes in a calcium-dependent manner (*21,22*). The imaging of acute cell death has been shown using C2A labeled with fluorochromes, superparamagnetic contrast agents, and a radioisotope (*23–25*).

Being able to recognize both phosphatidylserine and phosphatidylinositides, the C2A may be a practical candidate for the imaging of cardiac apoptosis and necrosis as a single comprehensive category, thus estimating the overall irreversible myocardial damage. In cardiomyocyte membranes, anionic phospholipids account for about 7% of total phospholipid content, of which one third is phosphatidylserine and the dominant majority are phosphatidylinositides (*26,27*). Recently, we have demonstrated a prominent hot-spot uptake that was consistently detected in a rat model of myocardial ischemia and reperfusion (*25*). The aim of this study was to investigate the temporal and spatial uptake profile of ^{99m}Tc-C2A in the area at risk after ischemia and reperfusion. The outcome of this study will help determine the optimal imaging window and better define the molecular probe in detecting acute cardiac cell death.

MATERIALS AND METHODS

^{99m}Tc Labeling

The fusion protein of C2A and glutathione-s-transferase (C2A-GST) was overexpressed in *Escherichia coli,* purified, and labeled with ^{99m}Tc in a 2-step process, as described in detail previously (*25*). First, 200 μL of C2A-GST (2 mg/mL) were dissolved in phosphate-buffered saline (PBS) and mixed with 2 μL of 2-iminothiolane (10 mg/mL in dimethyl sulfoxide). The mixture was incubated at 37°C for 1 h. Five hundred microliters of $^{99m}TcO_4^-$ in 0.9% NaCl were added to a stannous glucoheptonate mixture (80 μg $SnCl_2$ vs. 8 mg sodium glucoheptonate). The reaction was kept under an N_2 stream for 10 min at room temperature. Four hundred microliters of ^{99m}Tc-glucoheptonate were then mixed with 200 μL of thiolated C2A-GST. The mixture was incubated at room temperature for 30 min and purified using a PD-10 column containing Sephadex G-25 (GE Healthcare) preequilibrated with PBS, pH 7.4. The protein concentration was determined by the Bradford method (BioRad).

AMI Model

This study was approved by the Institutional Animal Care and Use Committee under the guideline of the National Institutes of Health. Male Sprague–Dawley rats were anesthetized with sodium pentobarbital (50 mg/kg body weight) intraperitoneally. After tracheotomy and intubation, respiration was maintained using a rodent ventilator. The proximal left anterior descending coronary artery was occluded using a 6.0 suture at 1 mm below the left atrial appendage. For sham operation, the suture was only passed underneath the left anterior descending coronary artery, without ligation. The presence of acute ischemia/reperfusion was confirmed by the pale appearance of the area at risk and changes in electrocardiography profiles, including an immediate elevation of the ST segment and a significant increase in the amplitude and width of the QRS complex. After reperfusion, the chest wall was closed and ventilation was maintained until the rat could regain spontaneous respiration. The loose suture was left in place for staining of the area at risk.

Temporal Uptake of ^{99m}Tc-C2A-GST

The temporal uptake profile of ^{99m}Tc-C2A-GST in the area at risk was investigated by intravenously injecting ^{99m}Tc-C2A-GST at different time points after infarction (30-min ischemia), with the radioactivity in the area at risk directly quantified using γ-counting. In detail, ^{99m}Tc-C2A-GST (80 μg) was injected via a femoral vein catheter at 0, 1, 3, 6, and 24 h after reperfusion ($n = 4$ for each time point). Each rat was sacrificed at 1 h after injection, when, according to our previous studies, the uptake of the radiotracer would have reached a plateau and would have been minimally affected by blood-pool–related tracer kinetics (*23*). Although this protocol precludes uptake studies with a temporal resolution of less than 1 h, we believe that the protocol provides reliable measurements based on existing knowledge. Meanwhile, such temporal resolution is appropriate given that the progression of the pathophysiology of the postinfarction myocardium is in terms of hours instead of minutes.

After thoracotomy, the coronary was reoccluded by tightening of the suture in place. The area at risk was delineated by the intravenous infusion of 2 mL of Evans blue (2% w/v in PBS, pH 7.4), which stains the normally perfused myocardium dark blue. The cardiac tissues from the area at risk were dissected and submerged in 2.5% triphenyl tetrazolium chloride (TTC) for 15 min at 37°C. Ischemic noninfarcted myocardium is stained brick red by TTC, whereas infarcted tissues are pale. TTC staining was not performed for the 0-h-after-reperfusion group, because TTC staining is not reliable until about 2 h after reperfusion. The dissected tissues for normal myocardium (blue), ischemic but viable myocardium (red), and infarcted myocardium (pale) were separately weighed and collected in sample tubes for γ-counting. Three aliquots of ^{99m}Tc-C2A-GST solution were measured for radioactivity as standards for the calculation of percentage injected dose (%ID). The uptake of ^{99m}Tc-C2A-GST at each time point after reperfusion was presented as %ID/g with SD.

Serial autoradiography was performed to confirm the above finding by demonstrating the dynamics of radiotracer uptake versus the duration of reperfusion. In detail, ^{99m}Tc-C2A (80 μg) was injected intravenously in infarcted rats (30 min of ischemia) at 1, 3, 6, and 24 h after reperfusion. The timing of ischemia was arranged to synchronize the radiotracer injection in all animals, so that each rat received an identical radiopharmaceutical dose. By synchronizing the radiotracer injection and sampling, this protocol was designed to eliminate the differences caused by the physical decay of the radioisotope. At 3 h after injection, all animals were sacrificed at the same time. Short-axis sections (0.5 mm thick) of the heart from the apex to the level of ligation were simultaneously exposed to BMX MS film (Kodak).

Alternatively, the radiotracer was injected at 2 h after reperfusion, and the uptake was measured at 1, 3, 6, and 24 h after injection. The radioactivity uptake in the infarcted, ischemic noninfarcted, and normal myocardium was quantified by γ-counting, as described above.

Planar Imaging

To confirm that the hot-spot uptake of ^{99m}Tc-C2A-GST on planar images is distributed specifically in the area at risk, and

predominantly in the infarcted tissues, coronary ischemia (30 min) was induced in rats ($n = 6$), followed by reperfusion. ^{99m}Tc-C2A-GST (80 μg) was injected intravenously at 2 h after reperfusion. An anterior planar image of each rat (prone position) was acquired at 3 h after radiotracer injection on an Infinia γ-camera (GE Healthcare) equipped with a high-resolution parallel-hole collimator, with a 15% energy window centering on 140 keV. The field of view was 22.5 × 22.5 mm, with a 512 × 512 matrix. Each image was acquired with 1 million counts. For confirmation of the distribution of radiotracer in cardiac tissues, each rat was sacrificed by intraperitoneal injection of an overdose of sodium pentobarbital (200 mg/kg). After thoracotomy, the heart was excised and rinsed in saline. Two milliliters of prewarmed TTC solution (2.5% w/v in PBS, pH 7.4) was infused into the entire myocardium in a retrograde fashion via the aorta. TTC staining was allowed to continue for 15 min at 37°C and was followed by retrograde infusion of 10 mL of formaldehyde (4% v/v in PBS, pH 7.4) to terminate the TTC reduction reaction and to preserve the tissue. The fixed heart was sectioned into consecutive 0.5-mm slices and exposed to BMX MS film. The tissue slices were then photographed in the same orientation as for the corresponding autoradiography.

Spatial Distribution of ^{99m}Tc-C2A-GST in Myocardium

This section was designed to investigate, when infarct size varied, the absolute radioactivity uptake in terms of %ID/g in the area at risk, infarcted myocardium, and ischemic noninfarcted myocardium after ischemia and reperfusion. In detail, 3 groups of rats (4 rats per group) underwent coronary ligation for 18, 22, and 30 min to induce various degrees of infarction while the area at risk remained constant. ^{99m}Tc-C2A-GST was injected intravenously via a femoral catheter at 2 h after reperfusion. At 3 h after injection, heart tissues were harvested and separated into infarcted and ischemic noninfarcted categories according to the staining protocol described above. After each sample had been weighed, the radioactivity level within the tissue was determined by direct γ-counting. The total injected dosage was derived by measuring, in triplets, the radioactivity from aliquots of ^{99m}Tc-C2A-GST solution with known volumes. Data output was presented in terms of %ID/g with SD.

RESULTS

Temporal Uptake of ^{99m}Tc-C2A-GST

Radioactivity uptake levels in the area at risk were quantified when ^{99m}Tc-C2A-GST was injected at different times after reperfusion. As summarized in Figure 1, when the tracer was injected immediately after reperfusion and sampled 1 h later, uptake in the area at risk was 2.05 ± 0.37 %ID/g. Because TTC staining is unreliable until 2 h after reperfusion, radioactivity measurements for the infarcted and ischemic noninfarcted myocardium were not available for this data point. When the tracer was injected at 1 h after reperfusion, the presence of radioactivity was measured as 2.36 ± 0.36 %ID/g in the area at risk. At this time point, the infarcted and ischemic noninfarcted myocardium contained 2.96 ± 0.45 %ID/g and 1.23 ± 0.36 %ID/g of radioactivity, respectively. The level of uptake remained similar at 3 h after reperfusion. These values were followed by a decline when the tracer was injected at 6 h after reperfusion. Overall uptake in the area at risk decreased to an average of 1.56% ± 0.22%. The decreasing trend continued, and at 24 h after reperfusion, tracer uptake was 1.02 ± 0.09 %ID/g, 1.15 ± 0.14 %ID/g, and 0.65 ± 0.07 %ID/g for the area at risk, infarcted myocardium, and ischemic noninfarcted myocardium, respectively. In parallel, the radioactivity uptake in the normal myocardium remained consistent at all time points, at an average of 0.18 ± 0.04 %ID/g. As seen in the autoradiographs in Figure 2, a marked decrease in signal intensity was clearly shown when ^{99m}Tc-C2A-GST was injected

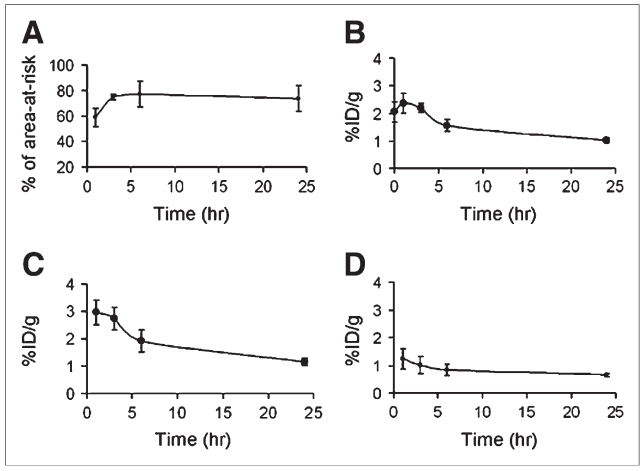

FIGURE 1. Temporal uptake profiles of ^{99m}Tc-C2A-GST in area at risk. ^{99m}Tc-C2A-GST was injected intravenously at 0, 1, 3, 6, and 24 h after reperfusion, and uptake of radioactivity was measured by γ-counting at 1 h after injection. (A) Changes in infarct size as percentage of area at risk. (B–D) Time-dependent uptake of radioactivity in area at risk (B), infarcted myocardium (C), and ischemic noninfarcted myocardium (D), in terms of %ID/g with SD ($n = 4$ for each group). Because TTC staining is unreliable less than 2 h after reperfusion, measurements for infarcted and ischemic noninfarcted myocardium were unavailable for first time point, for which injection and sampling were performed at 0 and 1 h after reperfusion, respectively.

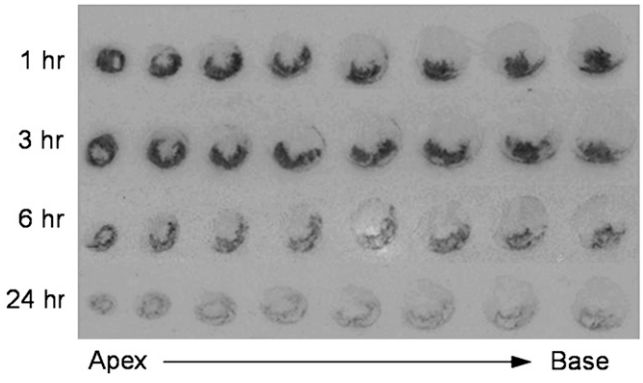

FIGURE 2. Autoradiographs of sections of infarcted hearts (30 min of ischemia). ^{99m}Tc-C2A-GST was injected intravenously at 1, 3, 6 and 24 h after reperfusion in separate rats. At 1 h after injection, short-axis sections (0.5-mm thickness) of each heart from apex to level of ligation were used to expose BMX MS film. Relative level of radioactivity uptake is qualitatively reflected by intensity of autoradiographs.

at 6 h after reperfusion, compared with 1 and 3 h. Uptake was further reduced when the radiotracer was injected at 24 h after reperfusion. Interestingly, when the tracer was injected early (2 h) after reperfusion, it was retained in the infarcted tissues with little washout (less than 10%) for at least 24 h (Fig. 3).

Planar Imaging

Well-defined focal uptake of the radiotracer was prominent in 6 of 6 cases of ischemia and reperfusion. An example whole-body anterior planar image is shown in Figure 4. This uptake profile was absent in sham-operated rats, which underwent an identical surgical procedure except for tightening of the suture over the coronary artery. In autoradiography, visual inspection indicated that the distribution of radioactivity consistently coregistered with the infarcted regions. In essence, there was not a single case of mismatch. As shown in Figure 4, the infarcted regions, which were stained negatively by TTC, were clearly identifiable as highly exposed areas in the corresponding autoradiographic films. The location and shape closely matched the stained histology sections. A consistent coregistration between histology and autoradiography is seen not only at the myocardial wall but also in the papillary muscles (Fig. 4, inset). From this collection of autoradiographs, it becomes apparent that the radioactivity was distributed predominantly in the infarcted tissues. On the other hand, normal remote myocardium appears to have a rather low radioactivity uptake, thereby facilitating a sharp target-to-background contrast. These qualitative observations are to be further investigated quantitatively in the next section.

Spatial Distribution of ^{99m}Tc-C2A-GST in Heart

For quantitative characterization of the spatial distribution of radioactivity in the heart, cardiac tissues were analyzed at 3 h after injection. There was no significant difference in the size of the area at risk among all 3 groups, at 47.2% ± 2.8%, 47.7% ± 8.3%, and 50.3% ± 8.4% of the left ventricle, reflecting a consistency in the coronary ligation technique. As expected, the infarct size increased with prolonged ischemia from 37.7% ± 14.6% to 65.6% ± 9.8% and to 77.5% ± 2.6% of the area at risk with 18, 22, and 30 min of ischemia, respectively. Consistent with the autoradiography, the radioactivity colocalized predominantly with the infarcted region. The spatial distribution data are summarized in Figure 5.

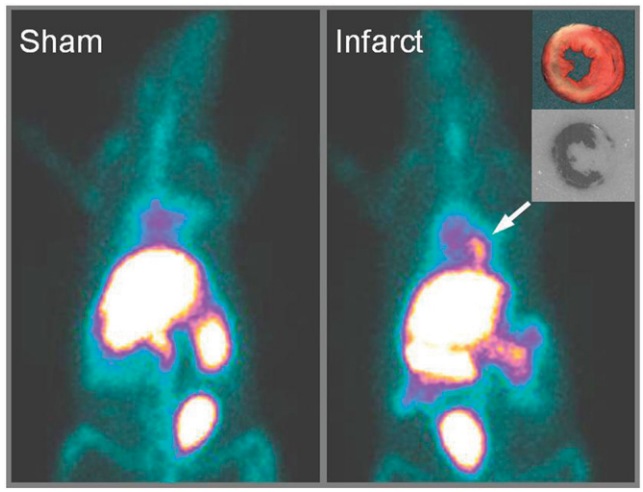

FIGURE 4. Representative anterior planar imaging of sham-operated control rat (left) and rat with ischemia/reperfusion (right). ^{99m}Tc-C2A-GST was injected intravenously at 2 h after reperfusion, and images were acquired at 3 h after injection. Distribution of radioactivity was confirmed postmortem by autoradiography, which is shown with corresponding TTC-stained tissue section (inset).

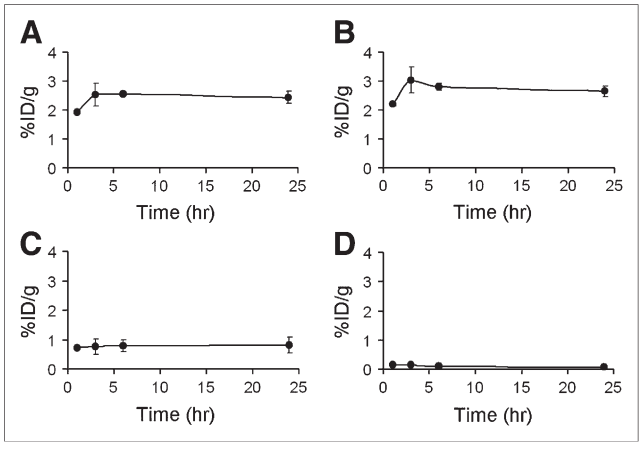

FIGURE 3. Radioactivity uptake in area at risk at 0, 1, 3, 6, and 24 h after ^{99m}Tc-C2A-GST was injected at 2 h after reperfusion. Time-dependent uptake of radioactivity, measured by quantitative γ-counting, in area at risk (A), infarcted myocardium (B), ischemic noninfarcted myocardium (C), and normal myocardium (D) is shown in terms of %ID/g with SD (n = 4 for each group).

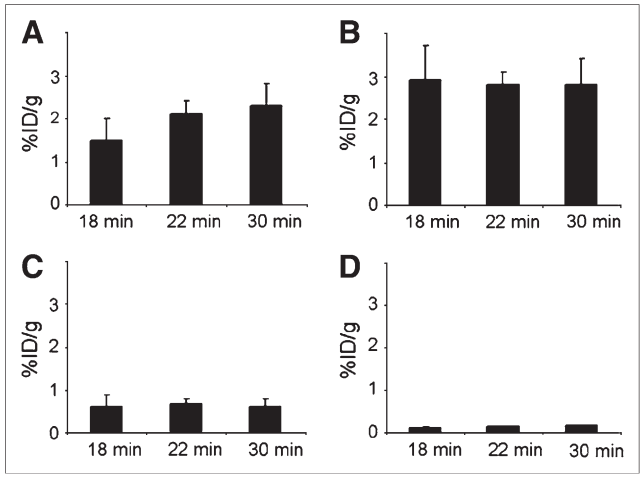

FIGURE 5. Spatial distribution of ^{99m}Tc-C2A-GST uptake in area at risk. Various degrees of ischemic injury were induced by occluding left anterior descending coronary artery in different groups of rats for 18, 22, and 30 min. Absolute uptake of radioactivity was determined by γ-counting and documented for area at risk (A), infarcted myocardium (B), ischemic noninfarcted myocardium (C), and normal myocardium (D) in terms of %ID/g with SD (n = 4 for each group).

With increasing ischemic durations, there was an overall increase in radioactivity uptake in the area at risk. However, a closer analysis revealed that the absolute radiotracer uptake in the infarcted and ischemic noninfarcted tissues, in terms of %ID/g, appeared to be independent of the ischemic duration. For instance, the absolute radioactivity level in the infarct was 2.9 ± 0.7, 2.8 ± 0.3, and 2.8 ± 0.5 for 18, 22, and 30 min of ischemia, respectively. In other words, a greater ischemic duration was reflected in the overall tracer uptake in the area at risk as a whole, instead of the absolute uptake levels in each type of pathologic tissue (i.e., infarcted and ischemic noninfarcted).

DISCUSSION

Based on our prior discovery that intense hot-spot uptake was consistently detected in a rat model of AMI, this investigation was designed to characterize the temporal and spatial distribution profiles of ^{99m}Tc-C2A-GST as a target-specific molecular probe in assessing acute cardiac cell death.

According to the current temporal uptake data, when the radiotracer is injected early (2 h) after reperfusion, it is retained in the infarcted tissues with little washout (less than 10%) for at least 24 h. However, if the injection is done at 6 or 24 h after reperfusion, the uptake in the infarct is already reduced by 30% or more than 50%, respectively. This finding may imply that the binding targets, presumably anionic phospholipids, are more accessible during an early window (1–3 h) after reperfusion and become partially concealed over time. In other words, the tracer molecules that are bound to the infarcted tissue early on remain bound inside the infarct, whereas those that are injected late have a more difficult time gaining access to the binding targets.

Drawing from the existing literature on the pathophysiology of the postinfarction myocardium, we may offer the following as a plausible underlying cause for the observed changes in tracer uptake as a function of time. The onset of AMI is accompanied by the exposure of high levels of anionic phospholipids. These molecular markers are externalized in apoptotic cells. In necrotic cells, the anionic phospholipids are readily accessible to the extracellular milieu. The uptake of ^{99m}Tc-C2A-GST in the early hours after reperfusion indicates a continuous availability of abundant binding targets in the dead and dying cardiac tissue. A subsequent decline in tracer uptake, when it is injected at or after 6 h after reperfusion, coincides with the timing at which the infarct size has become stabilized. These changes appear to take place in parallel with a continued deterioration of the myocardial endothelial functions due to reperfusion injury (*28–30*). In addition, AMI elicits an inflammatory response marked by neutrophil marginalization and infiltration of the necrotic site (*31,32*). This process is initiated by an overexpression of adhesion molecules on the endothelial surface, facilitating leukocyte recruitment and transmigration. Evidence has shown that the elevated neutrophil marginalization is associated with reduced perfusion, compounded by endothelial cell swelling and microvascular constriction after AMI (*31*). The reduced perfusion will, in turn, likely limit the delivery of the blood-borne radiotracer to the site of cell death, thus compromising the accessibility of the potential binding targets.

To evaluate the spatial distribution of radioactivity in the area at risk, we quantified the radioactivity uptake in the infarcted and ischemic noninfarcted myocardium using direct γ-counting. According to the current data, the intravenously injected radiotracer accumulates predominantly in the infarcted tissue, whereas uptake in the ischemic noninfarcted tissues was severalfold lower on a per-gram basis. The absolute tracer uptake, in terms of %ID/g, appears to be independent of infarct size. This uptake profile seems to be consistent with the pathophysiology of ischemically injured myocardium: Infarcted tissues are characterized by extensive necrosis, whereby molecular markers such as the anionic phospholipids are readily accessible to the extracellular environment. The relatively high abundance and availability of these binding targets are likely to have contributed to the prominent binding of the molecular probe. It is noteworthy that such uptake levels reflect specific binding, because our prior studies have shown that the passive distribution due to elevated vascular permeability would have been diminished from continuous washout (*25*). On the other hand, for ischemic noninfarcted myocardium, the uptake level is in line with the notion that the majority of cardiac cells retained viability (*2,3*). These quantitative uptake data may, in the long run, lead to not only the detection but also the noninvasive measurement of total cardiac cell death in the acute stage.

CONCLUSION

The temporal and spatial uptake of ^{99m}Tc-C2A-GST in the area at risk is dictated by the availability of binding targets and the pathophysiologic changes of the infarcted myocardium. The radiotracer is suitable for imaging cardiac cell death in the acute phase. Such an imaging technology will benefit the understanding of ischemic injuries to the myocardium and the investigation of cardioprotective treatments. In addition, C2A-GST as a cell death tracer could be of potential interest in pathologic conditions other than myocardial infarction, such as degenerative diseases and in the monitoring of tumor response to treatments.

ACKNOWLEDGMENTS

We thank Jundony Zhou and David Peck for technical assistance, Frank G. Steffel for administrative support, and Carrie M. O'Connor for editorial help. This work was supported in part by grant 0435147N from the American Heart Association.

REFERENCES

1. Braunwald E, Antman EM, Beasley JW, et al.; American College of Cardiology; American Heart Association; Committee on the Management of Patients with

Unstable Angina. ACC/AHA 2002 guideline update for the management of patients with unstable angina and non-ST-segment elevation myocardial infarction: summary article—a report of the American College of Cardiology/American Heart Association task force on practice guidelines (Committee on the Management of Patients with Unstable Angina). *J Am Coll Cardiol.* 2002;40:1366–1374.
2. Kostin S, Pool L, Elsasser A, et al. Myocytes die by multiple mechanisms in failing human hearts. *Circ Res.* 2003;92:715–724.
3. Freude B, Masters TN, Kostin S, et al. Cardiomyocyte apoptosis in acute and chronic conditions. *Basic Res Cardiol.* 1998;93:85–89.
4. Kerr JF, Wyllie AH, Currie AR. Apoptosis: a basic biological phenomenon with wide-ranging implications in tissue kinetics. *Br J Cancer.* 1972;26:239–257.
5. Song Z, Steller H. Death by design: mechanism and control of apoptosis. *Trends Cell Biol.* 1999;9:M49–M52.
6. Wyllie AH. Apoptosis: an overview. *Br Med Bull.* 1997;53:451–465.
7. Grutter MG. Caspases: key players in programmed cell death. *Curr Opin Struct Biol.* 2000;10:649–655.
8. Green DR. Apoptotic pathways: the roads to ruin. *Cell.* 1998;94:695–698.
9. Williamson P, Schlegel RA. Transbilayer phospholipid movement and the clearance of apoptotic cells. *Biochim Biophys Acta.* 2002;1585:53–63.
10. Fadok VA, Voelker DR, Campbell PA, Cohen JJ, Bratton DL, Henson PM. Exposure of phosphatidylserine on the surface of apoptotic lymphocytes triggers specific recognition and removal by macrophages. *J Immunol.* 1992;148:2207–2216.
11. Rucker-Martin C, Henaff M, Hatem SN, Delpy E, Mercadier JJ. Early redistribution of plasma membrane phosphatidylserine during apoptosis of adult rat ventricular myocytes in vitro. *Basic Res Cardiol.* 1999;94:171–179.
12. Huber R, Romisch J, Paques EP. The crystal and molecular structure of human annexin V, an anticoagulant protein that binds to calcium and membranes. *EMBO J.* 1990;9:3867–3874.
13. Blankenberg FG, Katsikis PD, Tait JF, et al. In vivo detection and imaging of phosphatidylserine expression during programmed cell death. *Proc Natl Acad Sci U S A.* 1998;95:6349–6354.
14. Ohtsuki K, Akashi K, Aoka Y, et al. Technetium-99m HYNIC-annexin V: a potential radiopharmaceutical for the in-vivo detection of apoptosis. *Eur J Nucl Med.* 1999;26:1251–1258.
15. Petrovsky A, Schellenberger E, Josephson L, et al. Near-infrared fluorescent imaging of tumor apoptosis. *Cancer Res.* 2003;63:1936–1942.
16. Lahorte CM, VanderHeyden JL, Steinmetz N, et al. Apoptosis-detecting radioligands: current state of the art and future perspectives. *Eur J Nucl Med Mol Imaging.* 2004;31:887–919.
17. Tait JF, Smith C, Blankenberg FG. Structural requirements for in vivo detection of cell death with ^{99m}Tc-annexin V. *J Nucl Med.* 2005;46:807–815.
18. Tait JF, Brown DS, Gibson DF, et al. Development and characterization of annexin V mutants with endogenous chelation sites for (99m)Tc. *Bioconjug Chem.* 2000;11:918–925.
19. Hofstra L, Liem IH, Dumont EA, et al. Visualisation of cell death in vivo in patients with acute myocardial infarction. *Lancet.* 2000;356:209–212.
20. Thimister PW, Hofstra L, Liem IH, et al. In vivo detection of cell death in the area at risk in acute myocardial infarction. *J Nucl Med.* 2003;44:391–396.
21. Zhang X, Rizo J, Sudhof TC. Mechanism of phospholipid binding by the C2A-domain of synaptotagmin I. *Biochemistry.* 1998;37:12395–12403.
22. Sutton RB, Davletov BA, Berghuis AM, Sudhof TC, Sprang SR. Structure of the first C2 domain of synaptotagmin I: a novel Ca2+/phospholipid-binding fold. *Cell.* 1995;80:929–938.
23. Zhao M, Beauregard DA, Loizou L, Brindle KM. Non-invasive detection of apoptosis using magnetic resonance imaging and a targeted contrast agent. *Nat Med.* 2001;7:1241–1244.
24. Jung HI, Kettunen MI, Davletov B, et al. Detection of apoptosis using the C2A domain of synaptotagmin I. *Bioconjug Chem.* 2004;15:983–987.
25. Zhao M, Zhu X, Ji S, et al. ^{99m}Tc labeled C2A domain of synaptotagmin I as a target-specific molecular probe for the non-invasive imaging of acute myocardial infarction. *J Nucl Med.* 2006;47:1367–1374.
26. Post JA, Langer GA, Op den Kamp JA, Verkleij AJ. Phospholipid asymmetry in cardiac sarcolemma: analysis of intact cells and 'gas-dissected' membranes. *Biochim Biophys Acta.* 1998;943:256–266.
27. Wheeldon LW, Schumert Z, Turner DA. Lipid composition of heart muscle homogenate. *J Lipid Res.* 1965;6:481–489.
28. Moens AL, Claeys MJ, Timmermans JP, Vrints CJ. Myocardial ischemia/reperfusion-injury, a clinical view on a complex pathophysiological process. *Int J Cardiol.* 2005;100:179–190.
29. Rochitte CE, Lima JA, Bluemke DA, et al. Magnitude and time course of microvascular obstruction and tissue injury after acute myocardial infarction. *Circulation.* 1998;98:1006–1014.
30. Luo AK, Wu KC. Imaging microvascular obstruction and its clinical significance following acute myocardial infarction. *Heart Fail Rev.* 2006;11:305–312.
31. Frangogiannis NG, Smith CW, Entman ML. The inflammatory response in myocardial infarction. *Cardiovasc Res.* 2002;53:31–47.
32. Go LO, Murry CE, Richard VJ, et al. Myocardial neutrophil accumulation during reperfusion after reversible or irreversible ischemic injury. *Am J Physiol.* 1998; 255:H1188–H1198.